Citation: M. Aranda, R. Aragüés, G. López-Nicolás. Shape Control of Maneuvering Planar Formations Based on Distributed Deformation Minimization. Robot 2023: Sixth Iberian Robotics Conference. ROBOT 2023. Lecture Notes in Networks and Systems, vol 976. Springer, Cham. 2024

Shape Control of Maneuvering Planar Formations Based on Distributed Deformation Minimization

Miguel Aranda, Rosario Aragüés, and Gonzalo López-Nicolás

Instituto de Investigación en Ingeniería de Aragón (I3A), Universidad de Zaragoza, E-50018 Zaragoza, Spain
{miguel.aranda,raragues,gonlopez}@unizar.es

Abstract. This paper presents a novel scheme for controlling planar multirobot formations. We assume the multirobot team's overall motion is guided by a subset of independently moving leader robots. We propose a strategy to control the other robots, called followers, based on minimizing a distributed deformation cost. This cost is based on a team organization in triads, i.e., three-robot subsets. Our strategy allows the team to maintain a prescribed formation shape while maneuvering under the leaders' guidance during, e.g., collaborative object transport or navigation tasks. We also study how to restrict the leaders' dynamics to facilitate formation tracking by the followers under motion constraints. The control laws we propose are distributed, can be designed locally, and rely on relative position measurements only. We illustrate our scheme with simulations considering single-integrator and unicycle robot dynamics.

Keywords: Multirobot systems · Deformation control · Mobile robots

1 Introduction

In various multirobot tasks such as object transport, navigation, and monitoring, a relevant goal is to keep the multirobot team close to a prescribed shape. In this paper, we propose a formation control strategy motivated by this goal. Formation control techniques [1] seek to maintain a certain geometric pattern specified via, e.g., relative inter-robot displacements [2], distances [3] or angular information [4]. Often, the team is required to maintain the pattern while simultaneously evolving dynamically according to task needs. To achieve this, a popular strategy is to use formation control with leader robots [4, 5]. Typically, the leaders control those team parameters not included in the formation specification, while the other robots (followers) have to stay close to that specification. Leader robots can generate, e.g., translation, rotation and scaling formation maneuvers, and even enforce affine deformations [6–8]. One alternative is to execute maneuvers in a leaderless fashion: for example, by purposeful design of the control parameters, one can obtain a desired dynamical evolution of the formation [9].

The approach we propose here is built on the work [10]. In this prior study, a team of robots grouped in sets of three (triads) achieved a prescribed planar

formation up to translation, rotation and scaling. The control strategy consisted in minimizing a distributed deformation cost. The proposed controller was leaderless, and the achieved formation was static. Here, in contrast, we present a control scheme with multiple leaders that allows the formation to maneuver dynamically. This is a key capability in various tasks, as mentioned above. The leaders' motions, which dictate the formation's translation, rotation and scaling, are considered exogenous and not controlled by us. What we propose is a control strategy for the followers, based on [10], which allows the full team to stay close to the prescribed formation shape during maneuvering. The main new contents we present are: (i) a characterization of how the positions of two leaders uniquely specify a formation with the prescribed shape for the full team, (ii) control laws for the followers so that they track that formation while minimizing team deformation, and (iii) a study on how to define dynamic bounds for the leaders to facilitate tracking by the followers. Our control laws use relative position measurements only, and are distributed and computable in local frames. We present illustrative simulations with single-integrator and unicycle robots.

Other approaches closely related to ours are those based on a complex-valued graph Laplacian, e.g., in [2, 6, 9, 11–13]. Analogously to [10], these studies propose control laws for planar formations with translation, rotation and scaling degrees of freedom. To fix these degrees of freedom, two leader robots are used in [13]. In [6], these two leaders are specifically employed to translate and resize the formation, while [9] considers leaderless maneuvers. Compared to these works, our controller minimizes deformation explicitly, which is a well-suited strategy for shape control in, e.g., deformable object transport [14], and we study specifically dynamic constraints from leaders to followers. The work [15] considers leader-follower formations with triangulated graphs (related to our triad structuring), but defines more restrictive graph conditions than us and a formation that cannot be scaled. Affine maneuvering [8] enables translation, rotation, scaling, and also affine deformation of a formation, which provides great maneuvering flexibility. The problem we target here (shape control) is different, and we use fewer (two) leaders; affine maneuvering requires at least three for a planar formation. Finally, a key distinguishing feature, inherited from [10], is that our control laws can be designed locally from geometric information: differently from [2, 6, 8, 9, 11–13], we do not need a centralized design of a control/stress matrix.

2 Problem Definition

Let $\otimes$, $\mathbf{1}_n$, $\mathbf{I}_n$, $||\cdot||$, and $(\cdot)^{(m)}$ denote respectively the Kronecker product, a column vector of n ones, the $n \times n$ identity matrix, the Euclidean norm, and the time derivative of order m. Let us consider a team of $n > 2$ robots in a planar workspace, with indices in the set $\mathcal{N} = \{1, ..., n\}$. We denote the team configuration at time t by $\mathbf{q}(t) = [\mathbf{q}_1^\intercal(t), ..., \mathbf{q}_n^\intercal(t)]^\intercal \in \mathbb{R}^{2n}$ where $\mathbf{q}_i(t) \in \mathbb{R}^2$ is robot i's position. We will often omit (t), for brevity. We define a *reference formation* for the team as a set of n constant positions, all different from one another and, without loss of generality, having zero centroid. We stack them

in $\mathbf{c} = [\mathbf{c}_1^\intercal, ..., \mathbf{c}_n^\intercal]^\intercal \in \mathbb{R}^{2n}$, where $\mathbf{c}_i \in \mathbb{R}^2$ denotes robot i's position in the reference formation. We model robot interconnections by an undirected static graph $\mathcal{G} = (\mathcal{N}, \mathcal{E})$. Each vertex corresponds to a robot, while an edge (i, j) in $\mathcal{E}$ indicates that the control law of i uses $j's$ relative position, and viceversa.

Our goal is for the team to maintain what we call the *shape condition* [10] while executing a collective motion task. This means that $\mathbf{q}$ is equal to $\mathbf{c}$ up to translation, rotation and uniform scaling. Defining $\mathbf{g_q} = [g_{qx}, g_{qy}]^\intercal \in \mathbb{R}^2$ as the centroid of $\mathbf{q}$, the shape condition implies that there exists a matrix $\mathbf{H}$ having the form $\mathbf{H} = [[h_1, h_2]^\intercal, [-h_2, h_1]^\intercal] \in \mathbb{R}^{2\times 2}$ such that $\mathbf{q}$ can be expressed as

$$\mathbf{q} = \mathbf{1}_n \otimes \mathbf{g_q} + (\mathbf{I}_n \otimes \mathbf{H})\mathbf{c}. \tag{1}$$

Observe that $(\mathbf{I}_n \otimes \mathbf{H})\mathbf{c}$ is a rotation and uniform scaling of the zero-centroid reference formation $\mathbf{c}$. To pursue the goal stated above, we build on the formulation of [10]. This formulation uses a distributed deformation cost γ_d to measure team shape error. This cost is defined as the sum of costs for triads, where a triad is defined as a set of three robots with a graph edge in $\mathcal{E}$ between every pair. In particular, $\mathcal{G}$ consists of interlaced triads and its structure satisfies the following requirements: every robot belongs to at least one triad; every triad has at least one other triad with which it shares two robots (we then say these two triads are interlaced); and there is a path of successive interlacings between any two triads. One possible structure complying with these requirements is a triangular mesh: as an example, bottom-left of Fig. 1 displays a reference formation with $n = 14$ robots and the edges of $\mathcal{G}$ for such a mesh; note that robots are labeled as leaders or followers, as will be explained in the next section.

The motivation for using the described triad-based graph structure is, first, that this can ensure shape convergence, i.e., convergence to a configuration satisfying (1), when using gradient descent on γ_d. Moreover, this graph structure has relevant advantages such as sparsity and modularity. We can express

$$\gamma_d = (-1/2)\mathbf{q}^\intercal \mathbf{A}_d \mathbf{q}, \quad -\nabla_{\mathbf{q}}\gamma_d = \mathbf{A}_d \mathbf{q}, \tag{2}$$

where $\mathbf{A}_d \in \mathbb{R}^{2n\times 2n}$ is a constant symmetric negative semidefinite matrix that encapsulates the reference formation and the triad structure. The Appendix provides more details of the formulation in [10]. The shape control strategy used in [10] was for the n robots to follow gradient descent on γ_d (2). This strategy was leaderless and the final configuration of the team was static, and it depended on the initial configuration. Here, we propose to use a similar shape control strategy, but we allow the formation to simultaneously maneuver. We achieve this via a leader-follower scheme, presented next.

3 Leader-Follower Control Scheme

We consider the team divided into $n_l \geq 2$ leaders and $n_f \geq 1$ followers, such that $n_l + n_f = n$. Their sets of indices are defined as $\mathcal{N}_l = \{1, ..., n_l\}, \mathcal{N}_f = \{n_l + 1, ..., n\}$, respectively. We express $\mathbf{q} = [\mathbf{q}_l^\intercal, \mathbf{q}_f^\intercal]^\intercal$ where $\mathbf{q}_l$ and $\mathbf{q}_f$ are respectively

$2n_l \times 1$ and $2n_f \times 1$ vectors containing the leader and follower positions. In this paper, we do not address the control of the leaders' motions, which are considered exogenous. We focus on controlling the followers, which will run gradient descent on γ_d (2). To formulate this, we will use a partition in blocks of $\mathbf{A}_d$, as

$$\mathbf{A}_d = \begin{bmatrix} \mathbf{A}_{ll} & \mathbf{A}_{lf} \\ \mathbf{A}_{fl} & \mathbf{A}_{ff} \end{bmatrix}, \text{ i.e., } \mathbf{A}_d\mathbf{q} = \begin{bmatrix} \mathbf{A}_{ll} & \mathbf{A}_{lf} \\ \mathbf{A}_{fl} & \mathbf{A}_{ff} \end{bmatrix} \begin{bmatrix} \mathbf{q}_l \\ \mathbf{q}_f \end{bmatrix}. \tag{3}$$

We assume the followers move according to single-integrator dynamics, i.e., $\dot{\mathbf{q}}_f(t) = \mathbf{u}_f(t)$, where $\mathbf{u}_f(t) = [\mathbf{u}_{n_l+1}^\intercal(t), ..., \mathbf{u}_n^\intercal(t)]^\intercal \in \mathbb{R}^{2n_f}$ is the control input for the set of followers and $\mathbf{u}_i(t) \in \mathbb{R}^2$ is robot i's control input.

3.1 Shape Control Conditions and Target Formation

Lemma 1. *The shape condition (1) holds if and only if* $\mathbf{A}_d\mathbf{q} = \mathbf{0}$.

Proof. From [10, Lem. 2], the shape condition holds if and only if $\gamma_d = 0$. *Note that* $\mathbf{A}_d\mathbf{q} = \mathbf{0}$ *implies* $\gamma_d = 0$ *(2). In addition, if* $\gamma_d = 0$, *as* $\mathbf{A}_d$ *is symmetric negative semidefinite, the gradient of* γ_d *is zero, i.e.,* $\mathbf{A}_d\mathbf{q} = \mathbf{0}$.

From this lemma, our control goal (1) is encapsulated by the constraint $\mathbf{A}_d\mathbf{q} = \mathbf{0}$. Hence, we will use this constraint to formulate our approach, relying on the properties of $\mathbf{A}_d$ and of its submatrices. We can write (1) as a linear combination of four linearly independent $2n$ vectors:

$$\mathbf{q} = g_{qx}(\mathbf{1}_n \otimes [1, 0]^\intercal) + g_{qy}(\mathbf{1}_n \otimes [0, 1]^\intercal) + h_1\mathbf{c} + h_2\mathbf{T}\mathbf{c}, \tag{4}$$

where $\mathbf{T} = \mathbf{I}_n \otimes [[0, 1]^\intercal, [-1, 0]^\intercal]$. Thus, from Lemma 1, the kernel of $\mathbf{A}_d$ has dimension four, and the rank of $\mathbf{A}_d$ is $2n - 4$. This same result was obtained in [2, 6, 11, 12] for a matrix playing an analogous role to our $\mathbf{A}_d$. For all subsequent developments in this paper, we assume the following.

Assumption 1 $\mathbf{A}_{ff}$ *is nonsingular.*

Analogous assumptions appear in related work on affine [8] or complex-Laplacian-based [6, 13] formation control, and on manipulation using an analogous modeling [16]. Considering the part of the right-hand side of $\mathbf{A}_d\mathbf{q} = \mathbf{0}$ that corresponds to the followers, we get, from (3), the constraint $\mathbf{A}_{fl}\mathbf{q}_l + \mathbf{A}_{ff}\mathbf{q}_f = \mathbf{0}$. If, per Assumption 1, $\mathbf{A}_{ff}$ is nonsingular, a given configuration $\mathbf{q}_l$ of the leaders defines a *unique* configuration for the followers that satisfies the above constraint. We name the unique positions in this configuration *follower setpoints*, $\mathbf{q}_{df} = [\mathbf{q}_{df(n_l+1)}^\intercal, ..., \mathbf{q}_{dfn}^\intercal]^\intercal \in \mathbb{R}^{2n_f}$. They are directly found as

$$\mathbf{q}_{df} = -\mathbf{A}_{ff}^{-1}\mathbf{A}_{fl}\mathbf{q}_l. \tag{5}$$

We then define, similarly to [8], the *target formation* as $\mathbf{q}^*(t) = [\mathbf{q}_l(t)^\intercal, \mathbf{q}_{df}(t)^\intercal]^\intercal \in \mathbb{R}^{2n}$. This is the unique team formation defined by the positions of the leaders at time t. Thus, what Assum. 1 means is that the leaders can dictate the configuration of the formation. As $\mathbf{A}_d$ is symmetric negative semidefinite (Sec. 2), its principal submatrices (which include $\mathbf{A}_{ff}$) are also symmetric negative semidefinite [17]. Therefore, from Assumption 1, $\mathbf{A}_{ff}$ is symmetric negative definite.

Proposition 1. *If $n_l = 2$, the target formation always satisfies the shape condition (1). Moreover, the scaling factor of this formation relative to the reference formation is nonzero if and only if the positions of the two leaders are different.*

Proof. Consider $\mathbf{q}_c^* = [\mathbf{q}_{cl}^{*\intercal}, \mathbf{q}_{cf}^{*\intercal}]^\intercal = \mathbf{A}_d\mathbf{q}^*$; from Lem. 1, showing $\mathbf{q}_c^* = \mathbf{0}$ will prove the result regarding the shape condition. Note $\mathbf{q}_{cf}^* = \mathbf{0}$, from (5). In addition, $\mathbf{q}_{cl}^* = (\mathbf{A}_{ll} - \mathbf{A}_{lf}\mathbf{A}_{ff}^{-1}\mathbf{A}_{fl})\mathbf{q}_l = (\mathbf{A}_d/\mathbf{A}_{ff})\mathbf{q}_l$, where $\mathbf{A}_d/\mathbf{A}_{ff}$ is the Schur complement of $\mathbf{A}_{ff}$ in $\mathbf{A}_d$. For $n_l = 2$ and due to Assumption 1, $\mathbf{A}_{ff}$ has rank $2n_f = 2n - 4$. This is equal to the rank of $\mathbf{A}_d$. Given that $rank(\mathbf{A}_d) = rank(\mathbf{A}_{ff}) + rank(\mathbf{A}_d/\mathbf{A}_{ff})$ [17], $\mathbf{A}_d/\mathbf{A}_{ff} = \mathbf{0}$; hence, $\mathbf{q}_{cl}^* = \mathbf{0}$, and $\mathbf{q}_c^* = \mathbf{0}$. Next, we prove the result regarding the scaling factor. As (1) holds, $\mathbf{q}^* = \mathbf{1}_n \otimes \mathbf{g}_\mathbf{q} + (\mathbf{I}_n \otimes \mathbf{H})\mathbf{c}$. Hence, for the two leaders' positions in the target formation we have $\mathbf{q}_2 - \mathbf{q}_1 = \mathbf{H}(\mathbf{c}_2 - \mathbf{c}_1)$ with $\mathbf{H} = [[h_1, h_2]^\intercal, [-h_2, h_1]^\intercal] \in \mathbb{R}^{2\times 2}$. The form of $\mathbf{H}$ implies that either $\mathbf{H} = \mathbf{0}$ or $\mathbf{H} = s_h\mathbf{R}_h \neq \mathbf{0}$ with $s_h > 0$ (scaling), $\mathbf{R}_h \in SO(2)$ (rotation). As $\mathbf{c}_2 - \mathbf{c}_1 \neq \mathbf{0}$, $\mathbf{q}_2 - \mathbf{q}_1 \neq \mathbf{0}$ implies $\mathbf{H} \neq \mathbf{0}$, and $\mathbf{H} \neq \mathbf{0}$ implies $\mathbf{q}_2 - \mathbf{q}_1 \neq \mathbf{0}$.

Prop. 1 means two leaders, at any two different positions, always define a target formation that has the shape of the reference formation. This is not the case if $n_l > 2$: the target formation may then be deformed. Note as well that Assum. 1 cannot hold if $n_l = 1$: this would imply $rank(\mathbf{A}_{ff}) = 2n-2$, which is impossible because $rank(\mathbf{A}_d) = 2n-4$ and $\mathbf{A}_{ff}$ is a submatrix of $\mathbf{A}_d$. Let us take $n_l = 2$ and group the parameters of (4) for the target formation as $\mathbf{w} = [g_{qx}, g_{qy}, h_1, h_2]^\intercal \in \mathbb{R}^4$. Let $\mathbf{S} = [[0, 1]^\intercal, [-1, 0]^\intercal]$ and recall that $\mathbf{c}_1$, $\mathbf{c}_2$ are the leaders' positions in $\mathbf{c}$. Next, we show how the leader positions $\mathbf{q}_l$ determine $\mathbf{w}$.

Proposition 2. *For $n_l = 2$, we have $\mathbf{w} = \mathbf{F}^{-1}\mathbf{q}_l$ with $\mathbf{F} \in \mathbb{R}^{4\times 4}$ having the form $\mathbf{F} = [[\mathbf{I}_2, \mathbf{I}_2]^\intercal, [\mathbf{c}_1^\intercal, \mathbf{c}_2^\intercal]^\intercal, [(\mathbf{S}\mathbf{c}_1)^\intercal, (\mathbf{S}\mathbf{c}_2)^\intercal]^\intercal]$.*

Proof. The $\mathbf{w}$ of the target formation for positions $\mathbf{q}_l = [\mathbf{q}_1^\intercal, \mathbf{q}_2^\intercal]^\intercal$ is found by imposing (4) on these positions. This can be expressed as $\mathbf{F}\mathbf{w} = \mathbf{q}_l$. One can find that $\det(\mathbf{F}) = \det([\mathbf{c}_{21}, \mathbf{S}\mathbf{c}_{21}]) = ||\mathbf{c}_{21}||^2$, where $\mathbf{c}_{21} = \mathbf{c}_2 - \mathbf{c}_1$. Hence, $\mathbf{F}$ is nonsingular, and $\mathbf{w} = \mathbf{F}^{-1}\mathbf{q}_l$.

This shows that by controlling their positions $\mathbf{q}_l$, the leaders can directly control $\mathbf{w}$ and thus maneuver (i.e., translate, rotate and resize) the target formation. Typically, the leaders are highly capable robots with detailed knowledge of the mission. The role of the leaders in our scheme may also be played by non-robotic entities (e.g., humans); this can be of interest in certain application scenarios.

3.2 Control Laws for the Followers

The followers' goal is to continuously track their setpoints $\mathbf{q}_{df}(t)$. For this, we can use the gradient descent control employed for the full team in [10]. Here we use it only for the followers. The control law, with a positive scalar gain k_P, is

$$\mathbf{u}_f = -k_P\nabla_{\mathbf{q}_f}\gamma_d = k_P(\mathbf{A}_{fl}\mathbf{q}_l + \mathbf{A}_{ff}\mathbf{q}_f). \tag{6}$$

Proposition 3. *Under (6), if the leaders are static, the positions of the followers converge globally to their setpoints.*

Proof. Let us define the tracking error as

$$\mathbf{e}_f = \mathbf{q}_f - \mathbf{q}_{df} = \mathbf{q}_f + \mathbf{A}_{ff}^{-1}\mathbf{A}_{fl}\mathbf{q}_l. \tag{7}$$

Multiplying by $\mathbf{A}_{ff}$*, we have* $\mathbf{A}_{ff}\mathbf{q}_f + \mathbf{A}_{fl}\mathbf{q}_l = \mathbf{A}_{ff}\mathbf{e}_f$*. In addition, as the leaders are static,* $\dot{\mathbf{q}}_{df} = \mathbf{0}$*. Hence,* $\dot{\mathbf{e}}_f = \dot{\mathbf{q}}_f$*. We can then substitute the control (6) to find* $\dot{\mathbf{e}}_f = k_P\mathbf{A}_{ff}\mathbf{e}_f$*. As* $\mathbf{A}_{ff}$ *is symmetric negative definite,* $\mathbf{e}_f$ *converges to zero globally, i.e.,* $\mathbf{q}_f$ *converges globally to* $\mathbf{q}_{df}$*.*

With persistent leader motions, the control law (6) will produce a non-vanishing tracking error $\mathbf{e}_f$, which can be reduced by increasing the value of k_P. To further improve tracking performance, we can use an integral term, $\mathbf{z}$, with a similar structure to those in, e.g., [6, 8, 11]. Concretely, we propose the control

$$\mathbf{u}_f = k_P(\mathbf{A}_{fl}\mathbf{q}_l + \mathbf{A}_{ff}\mathbf{q}_f) + k_I\mathbf{z}, \text{ with } k_P > 0 \in \mathbb{R},\ k_I > 0 \in \mathbb{R}, \tag{8}$$

$$\dot{\mathbf{z}} = \mathbf{A}_{fl}\mathbf{q}_l + \mathbf{A}_{ff}\mathbf{q}_f. \tag{9}$$

Proposition 4. *Under (8)-(9), if the leaders move with constant velocity, the positions of the followers converge globally to their setpoints.*

Proof. We can use again the tracking error $\mathbf{e}_f = \mathbf{q}_f - \mathbf{q}_{df} = \mathbf{q}_f + \mathbf{A}_{ff}^{-1}\mathbf{A}_{fl}\mathbf{q}_l$ *and the fact that* $\mathbf{A}_{ff}\mathbf{q}_f + \mathbf{A}_{fl}\mathbf{q}_l = \mathbf{A}_{ff}\mathbf{e}_f$*. The constant leader velocities* $\dot{\mathbf{q}}_l$ *represent a constant velocity of the follower setpoints:* $\dot{\mathbf{q}}_{df} = -\mathbf{A}_{ff}^{-1}\mathbf{A}_{fl}\dot{\mathbf{q}}_l$*. We have*

$$\begin{bmatrix}\dot{\mathbf{e}}_f \\ \dot{\mathbf{z}}\end{bmatrix} = \underbrace{\begin{bmatrix} k_P\mathbf{A}_{ff} & k_I\mathbf{I}_{2n_f} \\ \mathbf{A}_{ff} & \mathbf{0}_{2n_f\times 2n_f}\end{bmatrix}}_{\mathbf{A}_{PI}}\begin{bmatrix}\mathbf{e}_f \\ \mathbf{z}\end{bmatrix} + \begin{bmatrix}-\dot{\mathbf{q}}_{df} \\ \mathbf{0}_{2n_f\times 1}\end{bmatrix}. \tag{10}$$

Using properties of determinants of block matrices, the characteristic equation of $\mathbf{A}_{PI}$ *is* $\det(\lambda^2\mathbf{I}_{2n_f} - \lambda k_P\mathbf{A}_{ff} - k_I\mathbf{A}_{ff}) = 0$*. Following [11, Thm. 3, Cor. 1] where a similar system is analyzed, the eigenvalues* λ *of* $\mathbf{A}_{PI}$ *are the solutions of the equations* $\lambda^2 - k_P\mu_j\lambda - k_I\mu_j = 0$*, where* μ_j *for* $j \in \{1, ..., 2n_f\}$ *are the eigenvalues of* $\mathbf{A}_{ff}$*. As* $\mathbf{A}_{ff}$ *is symmetric negative definite, all* μ_j *are real and negative. From the Routh-Hurwitz criterion, all* λ *have negative real parts and the dynamics is stable. Hence, the system converges to a steady-state regime where*

$$k_P\mathbf{A}_{ff}\mathbf{e}_f + k_I\mathbf{z} - \dot{\mathbf{q}}_{df} = \mathbf{0}_{2n_f\times 1}, \tag{11}$$

$$\mathbf{A}_{ff}\mathbf{e}_f = \mathbf{0}_{2n_f\times 1}. \tag{12}$$

As $\mathbf{A}_{ff}$ *is nonsingular, (12) implies* $\mathbf{e}_f = \mathbf{0}$*, concluding the proof.*

Implementation of the Control. The requirements we pose on the followers are not high; in particular, note that the control laws (6), (8)-(9) are: (i) Distributed, i.e., each follower only needs to measure the relative positions of its neighbors in $\mathcal{G}$. (ii) Computed from position measurements only; using velocity feedback would improve tracking performance, but also increase complexity. (iii) Implementable by every follower using the measurements expressed in its own reference frame; we refer to the arguments on this last point given in [8, 10].

3.3 Analysis of Leader-to-Follower Dynamics

From (5), leader positions and follower setpoints are related as

$$\mathbf{q}_{df} = \mathbf{M}_{fl}\mathbf{q}_l, \text{ with } \mathbf{M}_{fl} = -\mathbf{A}_{ff}^{-1}\mathbf{A}_{fl}, \tag{13}$$

where we call the constant matrix $\mathbf{M}_{fl}$ of size $2n_f \times 2n_l$ the *mapping matrix*. We are interested in analyzing the leader-to-follower dynamics: i.e., how the follower setpoints change when the leaders move. This was addressed in [16] for first-order dynamics. Clearly, for any $m \in \mathbb{N}$, we have $\mathbf{q}_{df}^{(m)} = \mathbf{M}_{fl}\mathbf{q}_l^{(m)}$. Hence, the leader-to-follower dynamic relation is determined by the mapping matrix $\mathbf{M}_{fl}$. We study the structure of this matrix next. Consider the class of 2×2 real matrices having equal diagonal entries and opposite off-diagonal entries, i.e.,

$$\mathbf{M} = \begin{bmatrix} m_1 & -m_2 \\ m_2 & m_1 \end{bmatrix}, \text{ with } m_1, m_2 \in \mathbb{R}. \tag{14}$$

Any $\mathbf{M} \neq \mathbf{0}$ is a shape-preserving transformation that performs rotation and resizing and can be expressed as $\mathbf{M} = s\mathbf{R}$, with $s > 0$ being a scaling factor and $\mathbf{R} \in SO(2)$ a rotation. Next, we define a relevant class of matrices based on (14). We will use this definition in our subsequent analysis.

Definition 1. *We call a matrix of real numbers* $\mathbf{P}$ *of size* $2k \times 2l$, $k \geq 1$, $l \geq 1$ *an* ***RRM*** *if, when partitioned in* kl *blocks* $\mathbf{P}_{ij}$ *of size* 2×2, $i \in \{1, ..., k\}$, $j \in \{1, ..., l\}$, *i.e.,* $\mathbf{P} = [[\mathbf{P}_{11}^\intercal, ..., \mathbf{P}_{k1}^\intercal]^\intercal, ..., [\mathbf{P}_{1l}^\intercal, ..., \mathbf{P}_{kl}^\intercal]^\intercal]$, *every* $\mathbf{P}_{ij}$ *is a matrix of the class defined by (14).*

RR- in the name RRM alludes to *R*otate and *R*esize, the operations done by the blocks. The following two lemmas can be proved with standard manipulations.

Lemma 2. *A linear combination or product of two RRMs is an RRM.*

Lemma 3. $\mathbf{A}_d$ *is an RRM.*

Note $\mathbf{A}_{ll}$, $\mathbf{A}_{lf}$, $\mathbf{A}_{fl}$ and $\mathbf{A}_{ff}$ are also RRMs, since they are all formed by blocks of $\mathbf{A}_d$ defined as the $\mathbf{P}_{ij}$ in Definition 1. The result on $\mathbf{M}_{fl}$ is presented next.

Proposition 5. *The mapping matrix* $\mathbf{M}_{fl}$ *is an RRM.*

Proof. Recall $\mathbf{M}_{fl} = -\mathbf{A}_{ff}^{-1}\mathbf{A}_{fl}$. *The core element of our proof is showing* $\mathbf{A}_{ff}^{-1}$ *is an RRM, which we will do by considering incrementally larger submatrices of* $\mathbf{A}_{ff}$. *For this, denote by* $\mathbf{A}_i$, $i \in \{1, ..., n_f\}$ *the principal submatrix of* $\mathbf{A}_{ff}$ *built from its first* $2i$ *rows and columns. Note that as* $\mathbf{A}_{ff}$ *is symmetric negative definite, all* $\mathbf{A}_i$ *are symmetric negative definite [17], i.e., nonsingular. In addition, all* $\mathbf{A}_i$ *are RRMs, as they consist of blocks of* $\mathbf{A}_{ff}$ *selected consistently with Definition 1. Note as well that for any nonsingular* 2×2 *RRM, its inverse is a* 2×2 *RRM. We can directly apply this to the* 2×2 *top-left corner submatrix,* $\mathbf{A}_1$. *If* $n_f > 1$, *we next consider the* 4×4 *matrix* $\mathbf{A}_2$. *We partition it using* $\mathbf{B}$, $\mathbf{C}$ *and* $\mathbf{D}$ *all of size* 2×2, *and then express its inverse as [18]*

$$\mathbf{A}_2 = \begin{bmatrix} \mathbf{A}_1 & \mathbf{B} \\ \mathbf{C} & \mathbf{D} \end{bmatrix}, \ \mathbf{A}_2^{-1} = \begin{bmatrix} \mathbf{A}_{2_{11}} & \mathbf{A}_{2_{12}} \\ \mathbf{A}_{2_{21}} & \mathbf{A}_{2_{22}} \end{bmatrix}, \text{ with} \tag{15}$$

$$\mathbf{A}_{2_{11}} = \mathbf{A}_1^{-1} + \mathbf{A}_1^{-1}\mathbf{B}(\mathbf{D} - \mathbf{C}\mathbf{A}_1^{-1}\mathbf{B})^{-1}\mathbf{C}\mathbf{A}_1^{-1}, \;\; \mathbf{A}_{2_{12}} = -\mathbf{A}_1^{-1}\mathbf{B}(\mathbf{D} - \mathbf{C}\mathbf{A}_1^{-1}\mathbf{B})^{-1},$$
$$\mathbf{A}_{2_{21}} = -(\mathbf{D} - \mathbf{C}\mathbf{A}_1^{-1}\mathbf{B})^{-1}\mathbf{C}\mathbf{A}_1^{-1}, \;\; \mathbf{A}_{2_{22}} = (\mathbf{D} - \mathbf{C}\mathbf{A}_1^{-1}\mathbf{B})^{-1}. \tag{16}$$

Note all inverses in the four equations (16) exist. This is because $\mathbf{A}_2$ *and* $\mathbf{A}_1$ *are nonsingular, and hence the Schur complement* $\mathbf{A}_2/\mathbf{A}_1 = \mathbf{D} - \mathbf{C}\mathbf{A}_1^{-1}\mathbf{B}$ *is also nonsingular [18]. Recall that* $\mathbf{A}_1^{-1}$ *is an RRM.* $\mathbf{B}$, $\mathbf{C}$ *and* $\mathbf{D}$ *are also RRMs, as they come from blocks of* $\mathbf{A}_{ff}$ *selected consistently with Definition 1. Hence,* $\mathbf{A}_2/\mathbf{A}_1$*, a linear combination of products of RRMs, is an RRM too per Lemma 2. Therefore,* $\mathbf{A}_2/\mathbf{A}_1$ *is a nonsingular* 2×2 *RRM. Hence, as seen above,* $(\mathbf{A}_2/\mathbf{A}_1)^{-1}$ *is an RRM. Therefore, equations (16) are linear combinations of products of RRMs, so they are RRMs per Lemma 2, and hence,* $\mathbf{A}_2^{-1}$ *in (15) is an RRM.*

If $n_f > 2$*, we repeat the procedure for* $j = 3, ..., n_f$ *defining* $\mathbf{A}_j$ *in step* j *from* $\mathbf{B}_j$, $\mathbf{C}_j$ *and* $\mathbf{D}_j$ *of respective sizes* $2(j-1)\times 2$, $2\times 2(j-1)$ *and* 2×2*, as*

$$\mathbf{A}_j = \begin{bmatrix} \mathbf{A}_{j-1} & \mathbf{B}_j \\ \mathbf{C}_j & \mathbf{D}_j \end{bmatrix}. \tag{17}$$

By induction, we reach step $j = n_f$*, for which* $\mathbf{A}_j = \mathbf{A}_{ff}$*. Hence,* $\mathbf{A}_{ff}^{-1}$ *is an RRM. Since* $\mathbf{A}_{fl}$ *is an RRM,* $\mathbf{M}_{fl} = -\mathbf{A}_{ff}^{-1}\mathbf{A}_{fl}$ *is an RRM per Lemma 2.*

3.4 Imposing Dynamic Bounds

Let us interpret $\mathbf{M}_{fl}$ as partitioned in $n_f n_l$ blocks of size 2×2 and denote by $\mathbf{M}_{ij}$ the block corresponding to follower $i \in \mathcal{N}_f$ and leader $j \in \mathcal{N}_l$. As the mapping matrix $\mathbf{M}_{fl}$ is an RRM (Prop. 5), we can express every nonzero $\mathbf{M}_{ij}$ as $\mathbf{M}_{ij} = s_{ij}\mathbf{R}_{ij}$ with $s_{ij} > 0$ and $\mathbf{R}_{ij} \in SO(2)$. Let us denote the maximum scaling by $\bar{s}_{ij} = \max_{ij} s_{ij}$. Recall $\mathbf{q}_{df}^{(m)} = \mathbf{M}_{fl}\mathbf{q}_l^{(m)}$. We have the following result.

Proposition 6. *For* $m \in \mathbb{N}$*, if leader dynamics satisfy* $||\mathbf{q}_i^{(m)}(t)|| \leq \bar{q}_{lm}(t)\ \forall i \in \mathcal{N}_l$*, then follower setpoint dynamics satisfy* $||\mathbf{q}_{dfi}^{(m)}(t)|| \leq n_l\bar{s}_{ij}\bar{q}_{lm}(t)\ \forall i \in \mathcal{N}_f$*.*

Proof. For any possible $\mathbf{M}_{fl}$ *with the considered block structure, we have for any follower* $i \in \mathcal{N}_f$ *that*

$$\mathbf{q}_{dfi}^{(m)} = \sum_{j\in\mathcal{N}_l} \mathbf{M}_{ij}\mathbf{q}_j^{(m)} = \sum_{j\in\mathcal{N}_l, \mathbf{M}_{ij}\neq\mathbf{0}} s_{ij}\mathbf{R}_{ij}\mathbf{q}_j^{(m)}. \tag{18}$$

As $||\mathbf{R}_{ij}\mathbf{q}_j^{(m)}|| = ||\mathbf{q}_j^{(m)}|| \leq \bar{q}_{lm}$ *and* $s_{ij} \leq \bar{s}_{ij}$*, the stated result follows.*

Prop. 6 gives us a way of facilitating tracking when the followers have significant motion constraints (e.g., saturation and nonholonomicity), by prescribing bounds on the dynamics of their setpoints. Suppose we want to prescribe the bounds

$$||\mathbf{q}_{dfi}^{(m)}(t)|| \leq \bar{q}_{dfm}\ \forall i \in \mathcal{N}_f,\ \forall t \geq 0, \text{ with } m \in \mathbb{N}, \tag{19}$$

for a chosen $\bar{q}_{dfm}$. We then have a result following immediately from Prop. 6.

Corollary 1. *If the leader dynamics satisfy* $||\mathbf{q}_i^{(m)}(t)|| \leq \bar{q}_{dfm}/(n_l\bar{s}_{ij})\ \forall i \in \mathcal{N}_l$*,* $\forall t \geq 0$*, the bounds (19) are satisfied.*

Hence, we can choose $\bar{q}_{dfm}$ based on the followers' motion constraints, and then ensure (19) is respected by imposing on the leaders the bounds of Cor. 1.

4 Simulation Examples

We test the controller (8)-(9) in two MATLAB simulation examples. In both cases, we define the graph $\mathcal{G}$ as a Delaunay triangulation of the reference formation. This is a commonly used mesh structure that conforms with the triad interlacing we require. In the first example, illustrated in Fig. 1, we consider fourteen robots in a circular formation. Two leaders, using their knowledge of the mission and of the environment, translate the formation while also performing resizing (which allows traversing a narrow passage) and rotation. We consider single-integrator kinematics for the followers, with velocity norm saturation of 1 m/s. To illustrate Cor. 1 numerically for this example, assume we prescribe the bounds (19) with $\bar{q}_{df1} = 1\,\text{m/s}$ to ensure the setpoints cannot change faster than the followers can move. From $\mathbf{M}_{fl}$, we can compute $\bar{s}_{ij} = 1.611$. Then, Cor. 1 guarantees that if the leaders satisfy the condition $||\mathbf{q}_i^{(1)}(t)|| \leq 0.310\,\text{m/s}$ $\forall i \in \mathcal{N}_l$ $\forall t \geq 0$, then the prescribed bounds are satisfied. Note that the leader velocities conform with this condition, as their maximum norm over time is 0.3 m/s. Computing the setpoint velocities during the task, we confirm that $\max_{i,t} ||\mathbf{q}_{df\,i}^{(1)}(t)|| = 0.331\,\text{m/s} < \bar{q}_{df1}$. Observe that the followers track their formation setpoints driving the error $\mathbf{e}_f$ towards zero in the segments where the leader velocities remain constant, as theoretically expected.

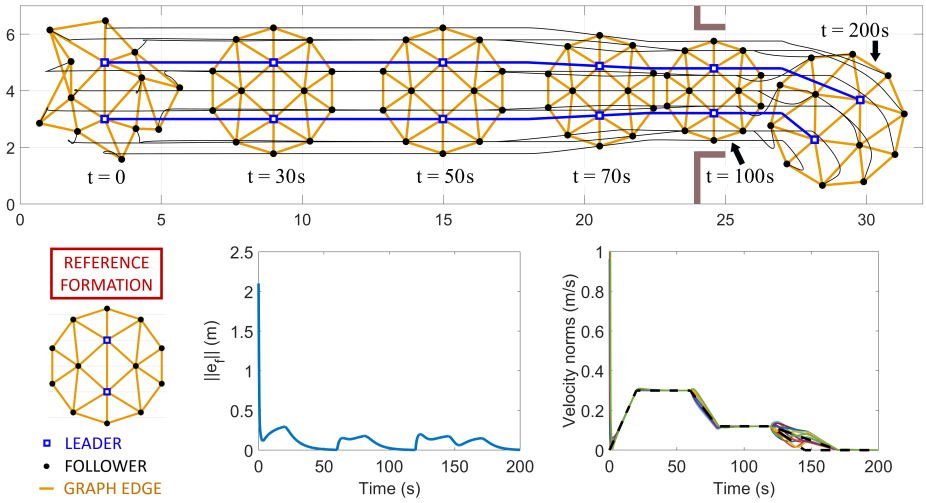

Fig. 1. Simulation results for the first example. Top: robot paths showing several intermediary team configurations with time stamps. The axes units are meters. A narrow passage appears at around $x = 25\,\text{m}$. Bottom, from left to right: legend for the plot on top, tracking error norm, and robot velocity norms, where dashed lines correspond to the leaders and solid lines correspond to the followers.

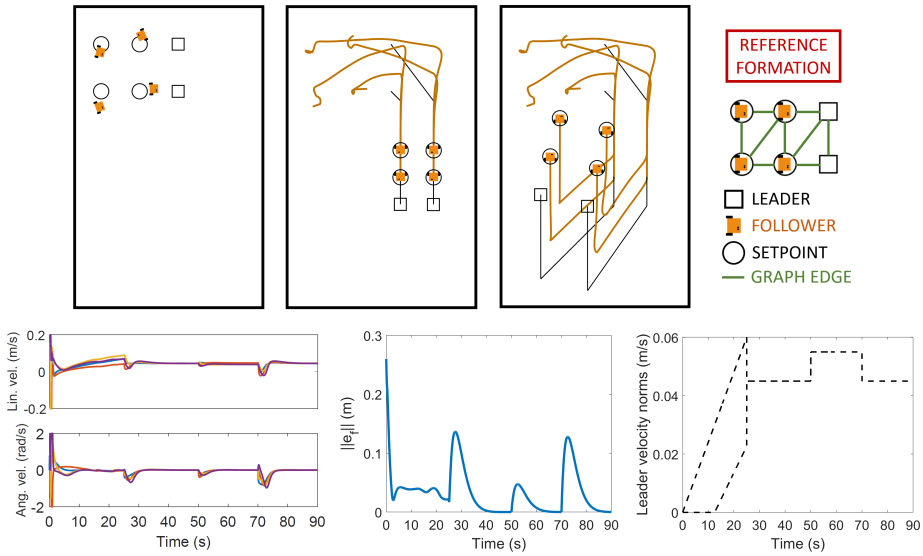

Fig. 2. Simulation results for the second example. On top row, from the left: initial configuration, intermediary configuration at $t = 49.5\,\text{s}$, and final configuration. The robot paths are also displayed. The size of the arena is $2\,\text{m} \times 3.2\,\text{m}$. The legend for these three plots is shown on the rightmost plot. Bottom, from left to right: unicycle velocities of the followers, tracking error norm, and leader velocity norms.

The second example, illustrated in Fig. 2, is executed on robots with unicycle kinematics in the MATLAB simulator of the Robotarium [19]. We use our single-integrator control law (8)-(9) which is converted to the linear and angular unicycle velocities [19]. Moreover, saturation of these velocities is considered. We define leader trajectories that translate, rotate, and resize the formation. The unicycle constraints make it more difficult for the followers to accurately track their setpoints, especially under sharp changes in the leaders' velocities. Still, a convergence behavior of $\mathbf{e}_f$ similar to the first example is observed. This second example thus illustrates the applicability of the proposed approach on robots with unicycle kinematics. Finally, we illustrate Prop. 6 in this example. We can take $\bar{q}_{l1}(t) = 0.06\,\text{m/s}\ \forall t \geq 0$. As $\bar{s}_{ij} = 1.918$, Prop. 6 ensures $||\mathbf{q}^{(1)}_{dfi}(t)|| \leq 0.230\,\text{m/s}$ $\forall i \in \mathcal{N}_f\ \forall t \geq 0$. This is satisfied, as $\max_{i,t} ||\mathbf{q}^{(1)}_{dfi}(t)|| = 0.090\,\text{m/s}$.

5 Conclusion

We presented a leader-follower controller to keep a team close to a reference formation shape while the team translates, rotates and changes its size during a mission. Our approach is simple in its design and implementation, and has interesting shape control properties. Topics of future work include higher-order robot dynamics, collision avoidance, and robustness to switching graph topologies.

Appendix: Formation Control From Triad-Based Deformation Cost

In [10], a deformation cost is defined for every triad in $\mathcal{G}$. This cost is the squared difference between current positions and optimally (in least-squares sense) translated, rotated and scaled reference positions for the three robots. γ_d is the aggregate of such costs. The control law for every robot $i \in \mathcal{N}$ follows the negative gradient of γ_d, as explained next. Denote by $\mathcal{T}_k$ a triad of index k, and by $\mathcal{N}_\mathcal{T}$ the set of all such indices. Let $\mathcal{N}_\mathcal{T}^i \subseteq \mathcal{N}_\mathcal{T}$ denote the set of indices of those triads that robot i belongs to. Further, let $\mathbf{q}_{0k}$ and $\mathbf{c}_{0k}$ denote the centroids for the triad $\mathcal{T}_k$: i.e., the centroids of the positions in $\mathbf{q}$ and in $\mathbf{c}$ of the three robots that form the triad $\mathcal{T}_k$. Then, considering robots with single-integrator kinematics, the control law $\mathbf{u}_i$ for robot i expressed in geometric terms is as follows [10]:

$$\mathbf{u}_i = \dot{\mathbf{q}}_i = \sum_{k \in \mathcal{N}_\mathcal{T}^i} \mathbf{H}_k(\mathbf{c}_i - \mathbf{c}_{0k}) - (\mathbf{q}_i - \mathbf{q}_{0k}), \ \ \forall i \in \mathcal{N}. \tag{20}$$

$\mathbf{H}_k \in \mathbb{R}^{2\times 2}$ is the optimal rotation and scaling transformation of the reference positions for $\mathcal{T}_k$, while the optimal translation component is handled by the centroid subtraction done in (20). In 2D, $\mathbf{H}_k$ is linear in $\mathbf{q}$; as a result, γ_d and its gradient have the simple expressions (2). The full team control law can thus be expressed as $\mathbf{u} = \dot{\mathbf{q}} = -\nabla_\mathbf{q}\gamma_d = \mathbf{A}_d\mathbf{q}$. Recalling $\mathbf{T} = \mathbf{I}_n \otimes [[0,1]^\intercal, [-1,0]^\intercal]$, $\mathbf{A}_d$ is expressed as follows, using $\mathbf{A}_k$, $\mathbf{L}_k$ of size $2n \times 2n$, $\mathbf{L}_{gk}$ of size $n \times n$:

$$\mathbf{A}_d = \sum_{k \in \mathcal{N}_\mathcal{T}} \mathbf{A}_k, \ \ \mathbf{A}_k = \frac{\mathbf{L}_k(\mathbf{c}\mathbf{c}^\intercal + \mathbf{T}\mathbf{c}\mathbf{c}^\intercal\mathbf{T}^\intercal)\mathbf{L}_k}{\mathbf{c}^\intercal\mathbf{L}_k\mathbf{c}} - \mathbf{L}_k, \tag{21}$$

$$\mathbf{L}_k = \mathbf{L}_{gk} \otimes \mathbf{I}_2, \, \mathbf{L}_{gk}[i,j] = \begin{cases} 2/3, & \text{if } i = j \ \& \ i \in \mathcal{T}_k \\ -1/3, & \text{if } i \neq j \ \& \ i,j \in \mathcal{T}_k \\ 0, & \text{otherwise.} \end{cases}$$

This control law is distributed: robot i needs to measure the relative positions of only those robots in triads that i belongs to. Also, i can express these measurements in its own reference frame, and the control law can be designed locally from geometric information, as shown by the expression (20).

Acknowledgement

This work was supported via projects PID2021-124137OB-I00 and TED2021-130224B-I00 funded by MCIN/AEI/10.13039/501100011033, by ERDF A way of making Europe and by the European Union NextGenerationEU/PRTR, via project REMAIN S1/1.1/E0111 (Interreg Sudoe Programme, ERDF), and via a María Zambrano fellowship funded by the Spanish Ministry of Universities and by the European Union-NextGenerationEU.

References

1. Oh, K.K., Park, M.C., Ahn, H.S.: A survey of multi-agent formation control. Automatica 53, 424–440 (2015)
2. Lin, Z., Wang, L., Han, Z., Fu, M.: Distributed formation control of multi-agent systems using complex Laplacian. IEEE Trans. Automat. Control 59(7), 1765–1777 (2014)
3. Mehdifar, F., Bechlioulis, C.P., Hashemzadeh, F., Baradarannia, M.: Prescribed performance distance-based formation control of multi-agent systems. Automatica 119, 109086 (2020)
4. Trinh, M.H., Zhao, S., Sun, Z., Zelazo, D., Anderson, B.D.O., Ahn, H.S.: Bearing-based formation control of a group of agents with leader-first follower structure. IEEE Trans. Automat. Control 64(2), 598–613 (2019)
5. Aldana-López, R., Gómez-Gutiérrez, D., Aragüés, R., Sagüés, C.: Dynamic consensus with prescribed convergence time for multileader formation tracking. IEEE Control Syst. Lett. 6, 3014–3019 (2022)
6. Han, Z., Wang, L., Lin, Z., Zheng, R.: Formation control with size scaling via a complex Laplacian-based approach. IEEE Trans. Cybern. 46(10), 2348–2359 (2016)
7. Oh, K.K., Ahn, H.S.: Leader-follower type distance-based formation control of a group of autonomous agents. Int. J. Control Automat. Syst. 15, 1738–1745 (2017)
8. Zhao, S.: Affine formation maneuver control of multiagent systems. IEEE Trans. Autom. Control 63(12), 4140–4155 (2018)
9. Garcia de Marina, H.: Distributed formation maneuver control by manipulating the complex Laplacian. Automatica 132, 109813 (2021)
10. Aranda, M., López-Nicolás, G., Mezouar, Y.: Distributed linear control of multi-robot formations organized in triads. IEEE Robot. Autom. Lett. 6(4), 8498–8505 (2021)
11. Fathian, K., Summers, T.H., Gans, N.R.: Robust distributed formation control of agents with higher-order dynamics. IEEE Control Syst. Lett. 2(3), 495–500 (2018)
12. Fathian, K., Safaoui, S., Summers, T.H., Gans, N.R.: Robust distributed planar formation control for higher order holonomic and nonholonomic agents. IEEE Trans. Robot. 37(1), 185–205 (2021)
13. Lin, Z., Ding, W., Yan, G., Yu, C., Giua, A.: Leader–follower formation via complex Laplacian. Automatica 49(6), 1900–1906 (2013)
14. Herguedas, R., Aranda, M., López-Nicolás, G., Sagüés, C., Mezouar, Y.: Double-integrator multirobot control with uncoupled dynamics for transport of deformable objects. IEEE Robot. Autom. Lett. 8(11), 7623–7630 (2023)
15. Guo, J., Lin, Z., Cao, M., Yan, G.: Adaptive control schemes for mobile robot formations with triangularised structures. IET Control Theory Appl. 4, 1817–1827 (2010)
16. Aghajanzadeh, O., Aranda, M., López-Nicolás, G., Lenain, R., Mezouar, Y.: An offline geometric model for controlling the shape of elastic linear objects. In: IEEE/RSJ Int. Conf. Intell. Robots Syst. pp. 2175–2181 (2022)
17. Horn, R.A., Johnson, C.R.: Matrix Analysis. Cambridge University Press, 2 edn. (2012)
18. Guttman, L.: Enlargement methods for computing the inverse matrix. Ann. Math. Stat. 17(3), 336–343 (1946)
19. Wilson, S., Glotfelter, P., Wang, L., Mayya, S., Notomista, G., Mote, M., Egerstedt, M.: The Robotarium: Globally impactful opportunities, challenges, and lessons learned in remote-access, distributed control of multirobot systems. IEEE Control Syst. Mag. 40(1), 26–44 (2020)